Tryptophan Spectroscopy Studies and Black Lipid Bilayer Analysis Indicate that the Oligomeric Structure of Cry1Ab Toxin from *Bacillus thuringiensis* Is the Membrane-Insertion Intermediate†

Carolina Rausell,‡,§ Carlos Muñoz-Garay,‡,§ Raúl Miranda-CassoLuengo,‡ Isabel Gómez,‡ Enrique Rudiño-Piñera,‖ Mario Soberón,‡ and Alejandra Bravo*,‡

Departamento de Microbiología Molecular and Departamento de Reconocimiento Molecular y Bioestructura, Instituto de Biotecnología, Universidad Nacional Autónoma de México, Apdo postal 510-3, Cuernavaca 62250, Morelos, Mexico

Received August 26, 2003; Revised Manuscript Received November 10, 2003

ABSTRACT: During intoxication, the Cry protoxins must change from insoluble crystals into membrane-inserted toxins, which form ionic pores. Binding of Cry1A toxins to the cadherin receptor promotes the formation of a 250 kDa oligomer. In this work, we analyzed for the first time the structural changes presented by Cry1Ab toxin upon membrane insertion. Trp fluorescence of pure monomeric and oligomeric structures in solution and in a membrane-bound state was analyzed. Cry1Ab has nine Trp residues, seven of them in pore-forming domain I. Trp quenching analysis with iodide indicated that oligomerization caused a 27% reduction in the level of Trp exposed to the solvent. Most of the oligomeric structure (96%) inserts into the membrane as a function of the lipid:protein ratio, in contrast to the monomer (10%). Additionally, the membrane-associated oligomer presented a blue shift of 5 nm in λ_{max} of the emission spectrum, indicating a more hydrophobic environment for some Trp residues. In agreement with this, iodide was unable to quench the Trp of the membrane-bound oligomer, suggesting that a significant part of the protein may be buried in the membrane. Quenching analysis using brominated and spin-labeled phospholipids in the vesicles indicates that most of the Trp residues are located close to the membrane−water interface. Finally, ionic currents in black lipid bilayers revealed that the oligomeric structure has kinetics different from those of the monomer, producing stable channels with a high probability of being open in contrast to the monomer that exhibited unstable opening patterns. These data show that the oligomer, in contrast to the monomer, is able to interact efficiently with phospholipid membranes forming stable pores.

Bacillus thuringiensis (Bt)[1] bacteria produce insecticidal proteins (Cry) toxic to different insect species and nematodes (*1*). To exert their toxic effect, a transition from crystal inclusion protoxins to membrane-inserted activated toxins is required for formation of pores in the apical membrane of the insect midgut epithelial cells (*1*, *2*). The crystal inclusions ingested by the susceptible larvae dissolve in the alkaline environment of the larval midgut, thereby releasing soluble proteins of 130 kDa, in the case of Cry1A toxins. The inactive protoxins are then cleaved at specific sites by midgut proteases, yielding ~60 kDa protease resistant fragments, which then bind to specific membrane receptors (*2*, *3*). The Cry1A proteins bind to a 120 kDa aminopeptidase N (APN) (*4*) and to a 210 kDa cadherin protein (Bt-R_1) (*5*) in lepidopteran insects. After receptor binding, toxin insertion results in the formation of lytic pores in microvilli membranes that leads finally to ion leakage, cell lysis, and eventual insect death (*1*).

The toxin−receptor interaction has been shown to be a necessary step for an efficient proteolytic activation of Cry1A toxins. The binding of Cry1Ab toxin to the cadherin receptor promotes proteolytic processing of helix α-1 of the toxin and formation of a 250 kDa prepore structure (probably tetrameric) which has been suggested to be responsible for ionic pore formation (*6*). Intermolecular interaction of Cry1Ab monomers has been reported (*7*, *8*), and a tetrameric oligomer of Cry1Ac was also observed in synthetic membranes (*9*). Cry1Ab and Cry1Ac toxin mutants affected by oligomerization mapped in helix α-4, in helix α-5, and in the loop between helices α-2 and α-3, indicating that these regions might be involved in toxin oligomerization (*7*, *10*). Nevertheless, the structural changes of Cry toxins during oligomerization and insertion into the membrane have still not been identified. Also, the analysis of Cry1A ion channel currents has only been carried out in monomeric preparations of toxin; this has never been done with a pure preparation of the oligomeric structure.

† This work was partially supported by CONACyT Grant G36505-N, DGAPA-UNAM Grant IN216300, UC MEXUS-CONACYT, and U.S. Department of Agriculture Grant 2002-35302-12539.

* To whom correspondence should be addressed. Telephone: (52-777) 3291635. Fax: (52-777) 3172388. E-mail: bravo@ibt.unam.mx.

‡ Departamento de Microbiología Molecular.

§ These authors contributed equally to this work.

‖ Departamento de Reconocimiento Molecular y Bioestructura.

[1] Abbreviations: Bt, *Bacillus thuringiensis*; BBMV, brush border membrane vesicles; APN, aminopeptidase N; Bt-R_1, *Manduca sexta* cadherin receptor; PC, egg-derived phosphatidylcholine; PS, bovine brain-derived phosphatidylserine; SUV, small unilamellar vesicles; LUV, large unilamellar vesicles; PLB, planar lipid bilayers.

10.1021/bi035527d CCC: $27.50
Published on Web 12/12/2003

Intrinsic fluorescence spectroscopy of Trp is a valuable tool for studying the conformation of proteins and for assessing the environment of Trp residues by means of emission fluorescence spectra and quenching experiments. Chemical agents such as iodide (I^-) and acrylamide quench Trp fluorescence, and the extent of quenching depends on the exposure of the indol moiety to the solvent. Via analysis of the efficiency of quenching, alterations in the molecular environment of Trp residues due to conformational changes of the protein or to the interaction of soluble proteins with the membrane can be determined (*11*). However, the emission data alone cannot reveal the depth of Trp residues within the membrane, because they reflect a number of factors such as the contributions of nearby residues to local polarity, the degree of solvent relaxation, and polarization artifacts. Nevertheless, brominated and spin-labeled phospholipids are effective collisional quenchers of the indole group that have been extensively used for determining the position of Trp within the bilayer (*12*).

Several membrane proteins such as anion exchangers, bacterial multidrug resistance proteins, bacteriorhodopsin, the photosynthetic reaction center, the potassium channel from *Streptomyces lividans*, and bacterial porins are prone to placing the tryptophan (Trp) residues near the membrane−water interface of their transmembrane domains (*13*). It has been suggested that the flat rigid shape of Trp limits its access to the hydrocarbon core and its π electronic structure favors residing in the complex water−bilayer interface environment (*13*). The proposed role of interfacial aromatic residues is to anchor the transmembrane segments for their orientation into the membrane and also to introduce rigidity to the periphery of the transmembrane segments.

To characterize the insertion of Cry1Ab toxin into the membrane, we recorded the fluorescence status of the Trp residues in pure preparations of the monomeric and oligomeric structures of Cry1Ab toxin and analyzed their role in the interaction with the membrane. Cry1Ab toxin has nine Trp residues, seven of which are located in domain I, the pore-forming domain, and two in domain II that is involved in receptor recognition (*14*). Trp residues located in domain I are highly conserved in the family of three-domain Cry proteins, suggesting an important role of these residues in toxin activity. Quenching analysis of Trp fluorescence using aqueous soluble quenchers and membrane-bound quenchers was performed to compare the properties of the soluble and membrane-inserted forms of Cry1Ab toxin. The membrane insertion of the oligomeric and monomeric structures was also assessed by analysis of ionic currents in black lipid bilayers. The data provided in this study show that the oligomeric structure, in contrast to the monomeric form, is able to interact efficiently with phospholipid membranes forming stable pores. The I^- quenching analysis showed that Trp residues in the membrane-bound oligomer are buried. Finally, the brominated membrane probes suggested that the majority of Trp residues are located near the membrane−water interface. Our results show that the oligomeric structure of the toxin is important in the process of insertion of Cry toxin into the membrane. The oligomeric structure could be considered an intermediate in the process of membrane insertion since it is formed outside of the membrane, and the monomeric structure must proceed through the formation of the soluble oligomer to become membrane-insertion competent. This is one of the first biochemical studies analyzing the transition from the soluble Cry1Ab toxin to its membrane-bound ionic pore state.

EXPERIMENTAL PROCEDURES

Cry1Ab δ-Endotoxin Purification. Cry1Ab crystals were produced in the acrystalliferous *Bt* strain 407*cry*$^-$ transformed with the pHT315 plasmid (*15*) harboring the *cry*1Ab gene (pHT315-1Ab). The transformant strain was grown for 3 days at 29 °C in nutrient broth sporulation medium supplemented with 10 μg/mL erythromycin. After complete sporulation, crystals were purified with sucrose gradients as reported previously (*16*) and solubilized in extraction buffer [50 mM Na_2CO_3 (pH 10.5) and 0.2% β-mercaptoethanol]. Activation of protoxin was performed as described previously (*6*) by incubation for 1 h with scFv73 antibody and digestion with midgut juice in a mass ratio of 1:4 for 1 h at 37 °C. PMSF was added to a final concentration of 1 mM to stop proteolysis. Purification of monomeric and oligomeric structures of Cry1Ab toxin was achieved by size-exclusion chromatography with a Superdex 200 HR 10/30 (Amersham Pharmacia Biotech, Uppsala, Sweden) FPLC size-exclusion column as described previously (*6*).

Purification of the scFv73 Antibody. The scFv73 antibody was purified from *Escherichia coli* cells with a Ni−agarose column, as described previously (*6*).

Western Blot of Cry1Ab Toxin. Purified monomeric and oligomeric structures of Cry1Ab toxin were separated via SDS−PAGE and transferred onto a nitrocellulose membrane. Cry1Ab proteins were detected with polyclonal anti-Cry1Ab (1:10000, 1 h) and visualized with a goat anti-rabbit antibody coupled with horseradish peroxidase (Sigma, St. Louis, MO) (1:1000, 1 h), followed by SuperSignal chemiluminescence substrate (Pierce, Rockford, IL) as described by the manufacturers.

Preparation of Small Unilamellar Vesicles (SUV) and Large Unilamellar Vesicles (LUV). Lipids, egg-derived phosphatidylcholine (PC) or bovine brain-derived phosphatidylserine with PC (PS/PC, 3:7 ratio) from chloroform stocks (Avanti Polar Lipids, Alabaster, AL), were mixed in glass vials on a scale of 2.6 μmol total and dried by argon flow evaporation followed by overnight storage under vacuum to remove residual chloroform. The lipids were hydrated in 2.6 mL of 10 mM HEPES, 150 mM KCl buffer (pH 7.2) by vortexing.

To prepare SUV, the lipid suspension was subjected five times to sonication for 5 min in a Branson-1200 bath sonicator (Danbury, CT). To prepare LUV, the mixture was passed 16 times through a 100 nm pore polycarbonate membrane using the Avanti Mini-Extruder (Avanti Polar Lipids) at room temperature. Liposomes were used within 4−5 days of being prepared. Liposomes were always prepared by keeping the total lipid concentration at 1 mM irrespective of the lipid composition and diluted to the required concentration just before use.

Fluorescence Emission and Quenching. Experiments were carried out using an Aminco Bowman (Urbana, IL) luminescence steady-state fluorescence spectrometer. All measurements were taken in a 4 mm × 10 mm quartz cuvette at 22 °C. The excitation and emission slits were 4 nm. The excitation wavelength was set at 280 or 290 nm for KI

quenching experiments, and the emission spectrum was recorded from 300 to 400 nm. The spectra that are presented were averages of three to four scans and were also corrected for background and dilution.

Titration of the Trp fluorescence emission of the Cry1Ab oligomeric form with increasing concentrations of SUV or LUV was carried out by adding small-volume aliquots of stock SUV or LUV to the protein suspension in the cuvette. After liposome addition, incubation for 1 h at room temperature was allowed before the spectra were acquired. Finally, the membrane fraction was separated by ultracentrifugation (1 h at 100000*g*), and the fluorescence spectra were recorded in both fractions, supernatants and pellet (suspended in the same buffer volume). Controls of oligomeric and monomeric Cry1Ab incubated in the absence of a membrane were performed, showing that both protein structures remain in solution under these experimental conditions. Also, control spectra from SUV or LUV alone were performed under the same conditions and subtracted from the respective protein spectra.

Fluorescent Quenching Experiments Were Performed with I^- (KI) and Acrylamide. Small-volume aliquots of stock solutions, 4 M KI and 8 M acrylamide, prepared in the protein buffer were added to the samples and gently stirred. The emission spectra were recorded to check the effect on fluorescence intensity and λ_{max}. As a control in KI quenching assays, KCl was added so that the total salt (KI and KCl) concentration remained constant and equal to the highest concentration of KI used. Sodium thiosulfate (800 μM) was added to KI solutions to prevent the formation of I_3^-, which absorbs at the same wavelength of Trp.

Effective Stern−Volmer constants (K_{SV}) were obtained from the fluorescent data according to the Stern−Volmer equation for dynamic quenching (*11*):

$$F_o/F = 1 + K_{SV}[Q] \quad (1)$$

where F_o and F are the florescence intensities in the absence and presence of the quencher, respectively. The value for K_{SV} can be considered a reliable reflection of the bimolecular collisional constant for collisional quenching of the Trp since $K_{SV} = k_q\tau_o$, where k_q is the bimolecular collisional constant and τ_o is the lifetime constant in the absence of quencher. However, if all Trp residues are not equally accessible to the quencher, a modification of the Stern−Volmer plot can be described by the Lehrer equation (*11*):

$$F_o/(F_o - F) = 1/K_{SV}[Q] + 1/f_a \quad (2)$$

where $F_o - F$ refers to the change in fluorescence intensity on addition of the quencher and f_a refers to the fraction of Trp that is accessible to the quencher.

The quenching data with nitroxide spin-labeled phosphotempocholine (TEMPO-PC) and brominated phosphocholine (diBr-PC) lipids (Avanti Polar Lipids) are presented as the quenching efficiency defined as the ratio of the fluorescence in the presence of the quencher to that without (F_o) quencher by the relationship $[(\Delta F_o - \Delta F) \times 100]/\Delta F_o$, where ΔF_o and ΔF are the changes in fluorescence intensity upon binding of the protein to PC LUV and to liposomes containing the membrane-bound quenchers, respectively.

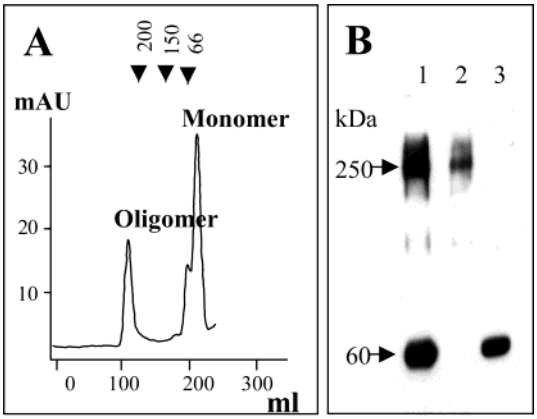

FIGURE 1: Purification of the oligomeric and monomeric forms of Cry1Ab toxin by size-exclusion chromatography. (A) Elution profiles of Cry toxin on a Superdex 200 HR 10/30 column. Arrowheads indicate the elution volumes of proteins with known molecular masses (shown in kilodaltons). (B) Western blot of purified monomeric and oligomeric structures of Cry1Ab toxin: lane 1, Cry1Ab protoxin proteolytically activated in the presence of the scFv73 antibody; lane 2, purified oligomeric structure after size-exclusion chromatography; and lane 3, purified monomeric structure after size-exclusion chromatography.

Protein Concentration. Protein concentrations were determined by two methods: (1) the Bradford assay using bovine serum albumin as a standard and (2) the extinction coefficient method in which $\epsilon_m^{280} = 5700\ M^{-1}\ cm^{-1}$ for Cry1Ab toxin.

Planar Lipid Bilayer Experiments. Planar lipid bilayers (PLB) were made by the method of Müeller and Rudin (*17*), with egg-derived PC (Avanti Polar Lipids, 20 mg/mL in *n*-decane). Typical bilayer capacitance values were between 250 and 350 pF. The buffer solution [300 mM KCl and 5 mM HEPES (pH 7.4)] was added to each of the cell compartments. Once the bilayer was formed, pure monomeric or oligomeric Cry1Ab toxins (1−300 nM) were added to the *cis* compartment; the *trans* compartment was held at virtual ground. All experiments were performed at room temperature.

Single-channel currents were recorded with a Dagan 3900A patch-clamp amplifier (Dagan Corp., Minneapolis, MN) as described in ref *18*. Currents were filtered at 200 or 500 Hz and digitalized on-line at 1 or 2 kHz, respectively, and analyzed on a personal computer using a Digidata 1200 interface and Axotape and pClamp software (Axon Instruments, Foster City, CA).

RESULTS

Steady-State Fluorescence Quenching of Trp Emission of Monomeric and Oligomeric Forms of Cry1Ab Toxin in an Aqueous Solution. Previous work demonstrated that a tetrameric oligomer was formed when Cry1Ab protoxin was proteolytically activated by midgut juice proteases in the presence of a single-chain antibody (scFv73) that mimics the Bt-R_1 receptor or by incubation with brush border membrane vesicles isolated in the absence of protease inhibitors (*6*). Cry1Ab protoxin was proteolytically activated in the presence of the scFv73 antibody, and the oligomeric and monomeric forms of the toxin were purified by size-exclusion chromatography as reported in Experimental Procedures. Figure 1A shows the elution profile from the

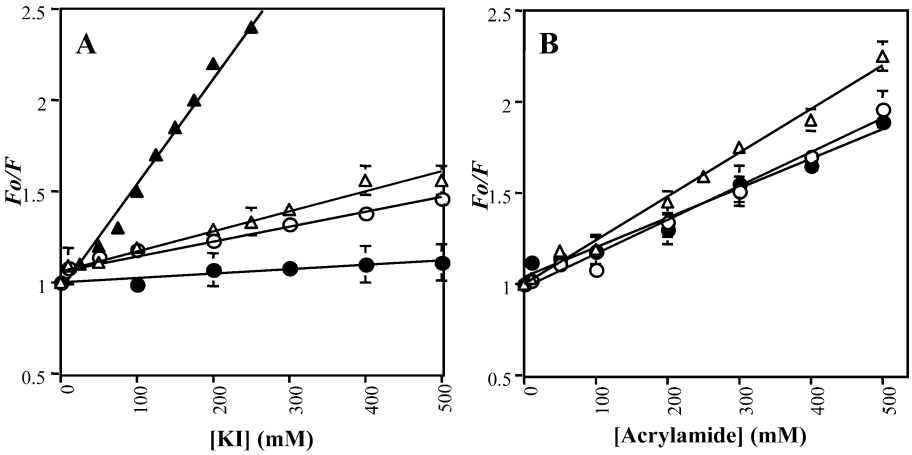

FIGURE 2: Stern−Volmer plots for (A) iodide and (B) acrylamide quenching of (▲) the denatured monomeric Cry1Ab toxin, (△) the monomeric Cry1Ab structure in solution, (○) the oligomeric Cry1Ab structure in solution, and (●) the oligomeric Cry1Ab structure inserted into phosphatidylcholine membrane vesicles. The intensity of maximal fluorescence emission was measured after excitation at 290 or 280 nm for KI or acrylamide quenching, respectively. F_o is the fluorescence intensity in the absence of the quencher, whereas F is the fluorescence intensity in the presence of the quencher. The SUV lipid:protein ratio was 5000.

Table 1: Comparison of the Cry1Ab Monomer and Oligomer Stern−Volmer Constants (K_{SV}) and Emission λ_{max} Values of the Trp Fluorescence in the Presence of Different Quenching Agents

	none	acrylamide		KI		
Cry1Ab structure	λ_{max} (nm)	$\lambda_{max}{}^a$ (nm)	K_{SV} (M^{-1})	$\lambda_{max}{}^a$ (nm)	K_{SV} (M^{-1})	Trp exp (%)
monomer in solution	336 ± 1.4	328 ± 1.6	2.50 ± 0.31	329 ± 0.6	1.15 ± 0.19	49.5 ± 9.4
oligomer in solution	333 ± 1.2	329 ± 1.4	1.88 ± 0.22	329 ± 0.6	0.83 ± 0.05	22.9 ± 1.7
oligomer in membrane	328 ± 0.6	328 ± 1.2	1.68 ± 0.06	328 ± 0.1	−	0

[a] Using the highest quencher concentration.

size-exclusion chromatography, and Figure 1B shows the Western blot analysis of the fractions containing the oligomeric and monomeric forms of Cry1Ab toxin. It is important to mention that as for the oligomer of aerolysin (*19*), pure preparations of the Cry1Ab oligomeric structure are unstable and tend to aggregate in a concentration-dependent manner (data not shown).

To analyze the interaction of the oligomeric and monomeric Cry1Ab with membrane vesicles, the Trp fluorescence of the two forms of the protein were analyzed first in the soluble state and then compared with that of membrane-associated proteins. The emission maxima of the native and denatured monomeric Cry1Ab toxin in 6 M guanidinium chloride (GndCl) were observed at 336 and 350 nm, respectively, indicating that some Trp residues were buried in the nonpolar interior of the toxin. We used I^- and acrylamide as quenchers of Trp fluorescence to obtain conclusions about the degree of Trp exposure. Both quenchers yielded linear Stern−Volmer plots (Figure 2). The apparent dynamic quenching constants K_{SV} derived from the slopes of these plots are presented in Table 1. In the case of quenching of the native monomeric toxin with I^-, 35.7% of the initial fluorescence was quenched at the highest quencher concentration, resulting in a blue shift in λ_{max} of 7 nm (Table 1). The effective K_{SV} for I^- quenching of the monomeric toxin was 1.15 M^{-1} (Figure 2A and Table 1). The Lehrer analysis gave an accessibility factor (f_a^{-1}) value of 2.02 ± 0.003, indicating that ~49.5 ± 9% of the Trp residues are accessible to I^-. These data agree with the crystallographic structure of the closely related Cry1Aa toxin (*14*) in which 57% of the Trp residues are exposed to the solvent as calculated with the InsightII program, where Trp219, -226, and -210 are highly exposed to the solvent followed by Trp73 and -117. These Trp residues are all located in domain I of Cry1Ab toxin. Trp219 and -226 are located in the loop between helices α-6 and α-7; Trp210 is located in helix α-6, Trp73 in helix α-2b, and Trp117 at the top of helix α-3. In the case of the 6 M GndCl-denatured toxin, 78% of the initial fluorescence was quenched with iodide. The analysis of these data using the Lehrer equation gave an f_a^{-1} value of 1.059 ± 0.0005, showing that 94.4 ± 3% of the Trp residues are accessible to quenching with I^- under denaturing conditions.

The oligomeric structure in solution exhibited maximal emission at 333 nm. The quenching analysis with I^- gave an effective K_{SV} constant of 0.83 M^{-1}, and a blue shift at the maximum quencher concentration of 4 nm, suggesting that Trp residues are less exposed to the solvent in the oligomer of Cry1Ab. The accessibility factor f_a^{-1} value of 4.367 ± 0.0006 indicated that only 22.9 ± 1.7% of the Trp residues of the oligomer are accessible to I^-. These data suggested that there is an important difference between the oligomeric and monomeric structures of Cry1Ab toxin, which involves a 27% reduction in the amount of Trp exposed to the solvent in the oligomeric structure.

To study the buried Trp residues in the monomeric and oligomeric structures of Cry1Ab, we used the neutral acrylamide quencher, which penetrates the interior of the protein and might quench some of the buried Trp (Figure 2B and Table 1). The Trp quenching analysis using acrylamide confirmed that the oligomeric structure has a different conformation resulting in lower exposure of some Trp residues to the solvent in comparison to the monomer.

Effects of Membrane Phospholipids on the Trp Fluorescence Emission of Monomeric and Oligomeric Structures of

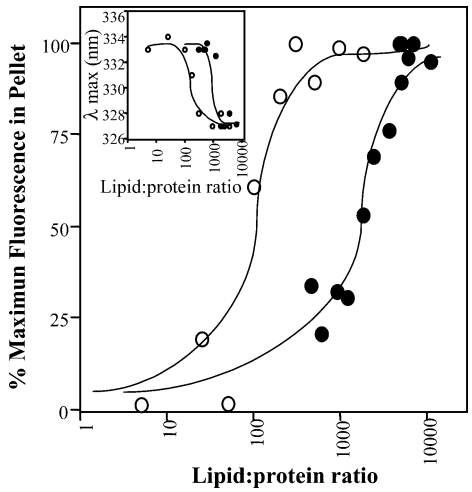

FIGURE 3: Binding of the oligomeric structure of Cry1Ab toxin to membranes. The percentage of maximum fluorescence recorded in the membrane pellet obtained after centrifugation for 1 h at 100000*g* of oligomeric Cry1Ab incubated with PC SUV (●) or LUV (○) as a function of lipid concentration. The inset shows the changes in maximal emission λ_{max} as a function of the lipid concentration. The protein concentration was kept constant, and the lipid:protein ratio is a molar ratio.

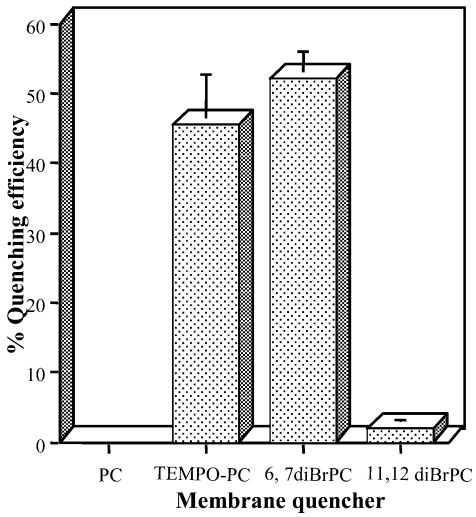

FIGURE 4: Quenching of the Cry1Ab oligomeric structure inserted in PC LUV in the presence of 10% membrane-bound quenchers, TEMPO-PC, 6,7-diBr-PC, or 11,12-diBr-PC. Quenching efficiencies were calculated from the oligomer fluorescence in PC LUV membranes with and without the lipid-bound quencher ($n = 3$).

Cry1Ab Toxin. Gómez et al. (*6*) reported that K^+ permeability in BBMV isolated from *Manduca sexta* was higher for the oligomeric than for the monomeric structure of Cry1Ab toxin, suggesting that there was a better interaction of oligomeric structures with the membrane (*6*). To analyze the interaction of both structures with the membrane, purified monomeric and oligomeric structures were incubated with phosphatidylcholine SUV or LUV. This membrane model was chosen because the interference with fluorescence emission is minimal between Trp and these vesicles, and also because previous studies demonstrated that Cry1 toxins are able to make pores in this membrane when used at high concentrations (*18*, *20*). SUV are extensively used because of their weaker scattering of light, but they are metastable and may produce anomalous peptide binding due to distorted lipid packing associated with high surface curvature. In contrast, LUV have a larger diameter and are in equilibrium, but they have stronger light scattering which may hinder both intensity and spectral measurement of Trp fluorescence (*21*). Due to these important differences between SUV and LUV and with the aim of avoiding misleading conclusions, we analyzed the insertion of Cry1Ab in both types of vesicles. Different lipid:protein ratios (from 1 to 10 000) were assayed with either the monomeric or oligomeric structures. After the incubation period, the membrane fraction was separated by ultracentrifugation and fluorescence spectra were recorded in both the supernatant and pellet fractions. Figure 3 shows that more than 96% of the protein from the oligomeric structure inserts into the membrane of SUV or LUV as a function of the lipid:protein ratio in contrast to Cry1Ab monomer, where only 10% was able to interact with the liposomes (data not shown). The threshold limit for partitioning of the oligomer into LUV or SUV was a lipid:protein ratio of 200 or 3000, respectively (Figure 3). The inset in Figure 3 shows the influence of an increasing concentration of total lipids on the Trp fluorescence emission of the oligomer. Insertion of the oligomeric structure in both membrane vesicles induced similar changes in the intensity and λ of the maximal emission.

The PC vesicles did not drastically affect the Trp fluorescence intensity of the oligomer, showing a maximum fluorescence enhancement of 20% when compared with that of the oligomer in solution and showing a blue shift of 5 nm in the emission spectrum λ_{max} from 333 nm in solution to 328 nm, indicating a more hydrophobic environment for some of the Trp residues. It has been described that changes in the fluorescence emission signature of the Trp residues of some proteins and peptides were only observed when the liposome mixture contained anionic lipids such as phosphatidylserine (PS) (*22*−*25*). To analyze the interaction of the oligomer with liposomes containing anionic lipids, we prepared SUV composed of a lipid mixture of PC and PS (7:3 ratio). The changes in Trp fluorescence intensity were subjected to saturation at a lipid:protein ratio of 5000 for this membrane composition, producing a maximum fluorescence enhancement of 89% and showing a blue shift of 6 nm in λ_{max}, very similar to the blue shift obtained in the PC SUV.

Effects of SUV on Trp Fluorescence Quenching of the Cry1Ab Oligomer. To further analyze the interaction of the oligomeric form of Cry1Ab toxin with the membrane vesicles, the accessibility of Trp residues in the presence of SUV was explored by fluorescence quenching. Steady-state fluorescence quenching was carried out using I^- and acrylamide (Figure 2A,B). I^- was unable to quench the Trp fluorescence of the oligomer inserted into the membrane, indicating that the Trp residues in the membrane-bound oligomer are strongly protected from exposure to the solvent.

Acrylamide is a neutral water-soluble quencher that has an advantage in that no electrostatic interactions take place with the headgroup of phospholipids and can permeate into hydrophobic environments. The quenching analysis carried out with acrylamide showed a K_{SV} value in the presence of PC SUV rather similar to the K_{SV} value obtained with the oligomer in an aqueous solution (Figure 2B and Table 1), suggesting that Trp residues are similarly accessible for quenching by acrylamide under both conditions.

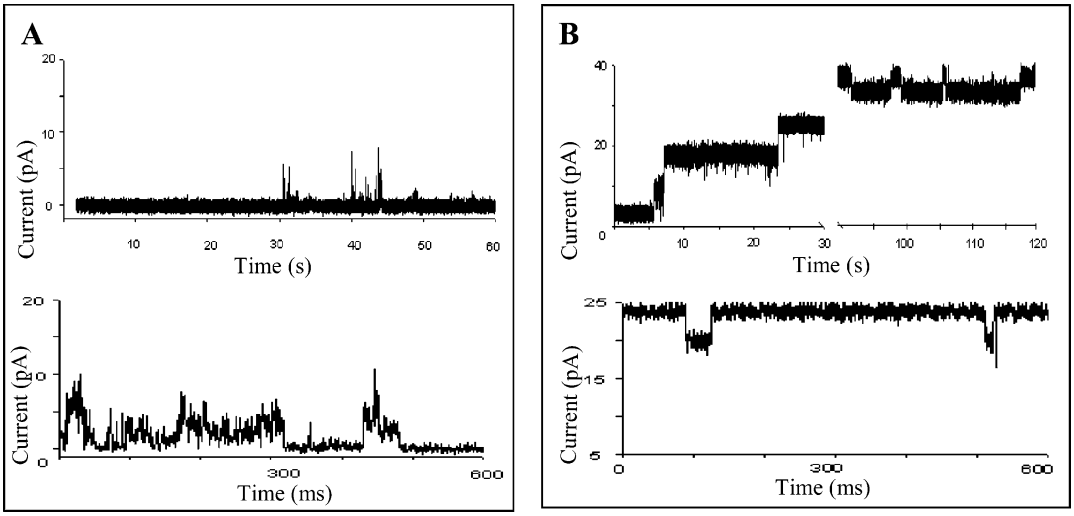

FIGURE 5: Representative ionic channel records of most common transitions induced in lipid bilayers by purified preparations of monomeric (A) or oligomeric (B) structures of Cry1Ab toxin. Records were obtained in 300 mM KCl and 5 mM HEPES (pH 7.4). The holding potential was 40 mV. The concentration of the monomeric structure was 150 nM and that of the oligomeric structure 6 nM.

Trp Fluorescence Quenching of Cry1Ab Toxin with Membrane-Bound Quenchers. Fluorescence quenching with I^- of the membrane-bound oligomer was consistent with the proposition that Trp residues were buried in the membrane. Additional support for the proximity of the oligomeric structure to the membrane lipids comes from data on quenching of Trp fluorescence with spin-labeled and brominated lipids at different positions on the acyl chain, i.e., TEMPO-PC-, 6,7-diBr-PC-, and 11,12-diBr-PC-containing LUV. Because these lipids are membrane-bound quenchers, comparison of their respective quenching ability yields information about the relative location of the Trp residues compared with the surface of the bilayer. Figure 4 shows that the presence of 10% spin-labeled or brominated PC in the vesicles induced a significant quenching of the Trp fluorescence of the oligomer. The magnitude of the quenching is greater when the doxyl group or the bromine atoms are located in the choline head (TEMPO), or positions 6 and 7 of the acyl chain with 48 and 55% of quenching efficiency, respectively, than when present at positions 11 and 12 where weak quenching was observed (Figure 4). These data are consistent with a location of the majority of the Trp residues of the oligomer close to the shallow quenchers, suggesting that they are located closer to the membrane−water interface, although the exact position of each Trp remains to be determined by using single-Trp mutants.

Responses of Oligomeric and Monomeric Cry1Ab Toxin in Planar Lipid Bilayers. To gain additional information about the insertion of Cry1Ab monomeric and oligomeric structures into the membrane, the induced ionic channel activities of pure monomeric or oligomeric structures were examined in synthetic planar lipid bilayers (PLB), and the main differences in the preliminary qualitative analysis of the induced channels are presented. These experiments were performed with equimolar KCl concentrations in both compartments. Channel activity induced by insertion of the Cry1Ab monomer was only observed at high toxin concentrations (>100 nM). The analysis of conductances of the pure monomeric Cry1Ab preparation was difficult because multiple subconducting states were present and also because the channels washed out, lasting only 1−2 min. Figure 5A illustrates the most frequent single-channel transitions detected in PLB in which pure monomeric Cry1Ab was incorporated. The single-channel transitions observed with 150 nM monomeric toxin were cationic and similar to those described previously (*18*, *20*).

The response of PLB after spontaneous Cry1Ab oligomer insertion was tested. The observed response involved multiple channels and a macroscopic conductance increase with some large single-channel transitions (Figure 5B). The induced response in bilayer experiments depends on toxin concentration, but the induction of channel activity by the oligomeric form of Cry1Ab was observed at a toxin concentration at least 20-fold lower than that of the monomeric Cry1Ab toxin. The oligomer forms stable channels as shown in the histogram of conductance amplitudes (Figure 6A) generated from 1 min macroscopic current records. In this figure, it is clear that the oligomeric structure showed a stable conductance state where the zero current state is absent. In contrast, the monomeric structure induced macroscopic currents with very unstable transitions showing multiple channels or subconductance stages. The quantitative analysis of the amplitude distributions showed two different substates with a difference of only 2 pA in the distribution of the oligomer-induced currents (labeled 6 and 7 in Figure 6A). The monomeric structure exhibited multiple substates with a broad distribution of amplitudes; the main populations had differences of at least 9 pA between them (labeled 1−4 in Figure 6A). From this histogram, we obtained the ratio of the total time spent in the open state by *N* different channels to the total recording time (NP_o, 1 min records). The oligomer-induced 30 pA amplitude exhibited an open probability of 0.85, indicating that this is the most stable open stage. In contrast, the monomeric structure induced channels with an overall open probability that varied from 0.05 to 0.4 with a tendency toward a gradual decrease in NP_o with an increase in amplitude (inset in Figure 6A).

The *I*−*V* curves of the oligomer-induced channels measured under symmetrical or gradient conditions (300 mM KCl or 100 mM *cis* and 300 mM *trans* KCl) indicate that the channels formed by the oligomeric form of the toxin are cationic with a P_{K^+}/P_{CL^-} of ∼3.5 (Figure 6B).

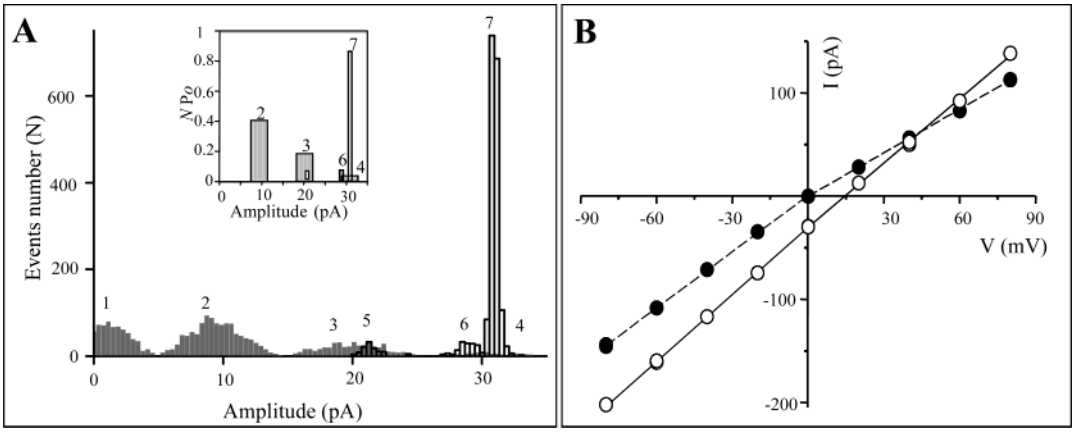

FIGURE 6: Analysis of channels induced by the oligomeric structure of Cry1Ab. (A) All-point current amplitudes histogram of 1 min macroscopic current recordings at 80 mV. Gray bars depict data from channels induced by the monomeric Cry1Ab toxin and white bars data from channels induced by the oligomeric Cry1Ab toxin. (B) Current−voltage (*I*−*V*) relationship of the macroscopic currents induced by the oligomeric Cry1Ab toxin measured under symmetrical 300 mM KCl (●) and 100 mM *cis* and 300 mM *trans* KCl gradient conditions (○). The inset in panel A shows the overall open probability of the channels. NP_o, the proportion of the total time spent in the open state by *N* different channels to the total recording time, was obtained for 1 min current records.

DISCUSSION

Cry protoxins must go through several structural changes before reaching their functional pore-forming state. These steps can be visualized as follows: (1) solubilization of the crystal and processing of the protoxin by midgut proteases, resulting in production of the monomeric toxin; (2) binding of the monomer to the cadherin receptor located in the apical membrane of midgut cells, probably accompanied by a mild denaturation of the monomer that allows the cleavage of helix α-1 (this cleavage might result in a conformational change and the formation of a molten globule state of the monomer with exposure of hydrophobic regions); (3) formation of a tetramer by intermonomeric contacts (toxin prepore), and (4) a second conformational change of the oligomer, resulting in the insertion into the membrane and formation of the membrane active pore.

The oligomeric structure of Cry1Ab-bound 8-anilino-1-naphthalenesulfonate ANS, which specifically reacts with solvent-accessible clusters of nonpolar residues, suggesting that Cry1Ab oligomerization after receptor binding is accompanied by the exposure of hydrophobic surfaces (*6*). The exposition of hydrophobic clusters could be related to the removal of helix α-1 that could expose either central hydrophobic helix α-5 or the hydrophobic surface of the other amphiphatic helices promoting the formation of the oligomeric active toxin. The oligomer that is formed is a stable structure since it is resistant to SDS treatment and boiling, suggesting a strong interaction between monomers (*6*, *7*, *10*).

Our studies reveal several features of the monomeric and oligomeric forms of Cry1Ab and the structural changes of the oligomeric structure occurring in the transition from the soluble to a membrane-bound form. In the monomer, the Trp residues were partially exposed to the solvent, as indicated by an emission maximum of 336 nm. The oligomer exhibited a maximum emission at 333 nm, suggesting a different conformation, where more Trp residues are buried in the protein. For comparison, Trp residues that are completely buried within globular proteins typically have emission maxima between 320 and 330 nm; those that are partially buried have maxima between 330 and 345 nm, and fully exposed Trp residues have maxima between 345 and 355 nm (*26*). Quenching studies using I^- and acrylamide supported this conclusion since K_{SV} values for the oligomer were lower than that of the monomer in solution (Table 1). The accessibility of Trp to water is generally thought to be the primary determinant of the K_{SV} constant in the Trp quenching by the anionic water-soluble I^-. Typically, fully exposed Trp residues have K_{SV} values of 8−9 M^{-1} (*27*), whereas K_{SV} values for buried or inaccessible Trp residues are lower and can be close to 0 M^{-1} (*28*). Upon binding to the membrane, the oligomeric structure goes through a conformational change where Trp residues are completely shielded as indicated by the inability of quenching with I^-. These data suggest that a significant part of the protein may be buried in the membrane. Other studies, like protease K protection assays of Cry1Ac bound to BBMV and scanning microcalorimetry studies of Cry3A toxin bound to liposomes, also suggested that most of the protein is inserted into the membrane (*7*, *29*). However, our study shows that most of the Trp residues of the membrane-bound oligomer are still accessible to acrylamide, suggesting that Trp residues are not deeply buried in the membrane. Studies of the quenching of Trp by acrylamide showed a linear dependence upon depth in the bilayer core. The Trp residues located at the surface of the bilayer are more sensitive to quenching by acrylamide, whereas the deep Trp residues are less sensitive to the quencher (*30*).

The depth of Trp residues in the membrane-bound oligomer was examined more directly using fluorescent quenching with spin-labeled and brominated lipids. Both of these phospholipids, when used as quenchers of Trp fluorescence, are good rulers for probing membrane insertion of peptides, because they act over a short distance, without drastically perturbing the membrane. Experiments with brominated and spin-labeled phospholipids further demonstrated that the most efficient quenching was obtained with the 6,7-diBrPC-containing and the TEMPO-PC-containing membranes. In the 6,7-diBrPC lipid, the bromines are 10.8 Å from the bilayer center, and in the TEMPO-PC lipid, the doxyl group is 20 Å away. The stronger quenching by the membrane-bound quenchers located near the lipid−water interface

suggests that the majority of Trp resideues are near this region. It is being more frequently recognized that Trp residues of membrane-bound proteins are preferentially located at the membrane−water interface. The membrane-bound form of Cry1Ab toxin thus appears to be another example of a protein whose aromatic residues seem to be sequestered in the membrane boundary. Other examples of pore-forming bacterial toxins that form oligomeric structures in the target membranes are aerolysin, perfingolysin O, and α-toxin (*31*). These toxins have Trp-rich domains that are involved in binding to their membrane receptors, and the Trp residues in these proteins are also located at the membrane−water interface (*31*). These data suggest that Trp residues may play an important role in the process of transforming water-soluble toxins into membrane-bound pores.

The pore formation activity of the oligomeric structure of the Cry1Ab toxin revealed kinetic characteristics different from those of monomeric Cry1Ab. These data suggest that the monomers do not assemble into oligomers within the membrane. The main difference between these structures besides the number of subunits is that monomeric structure harbors helix α-1 in contrast to the oligomeric structure, in which this helix was cleaved, and the cleavage of this helix has been proposed to be important for triggering oligomerization (*6*). The responses in PLB with oligomer preparations were observed at lower toxin concentrations than the responses with the monomer (20-fold). The oligomeric Cry1Ab exhibited more stable channels that had a high open probability in contrast to the monomeric toxin that exhibited an unstable opening pattern. The ion channels induced by various activated Cry1 toxins, including Cry1Aa (*14*, *32*), Cry1Ac (*32*−*34*), and Cry1C (*20*, *35*), have been analyzed in different zwitterionic membrane compositions in black lipid bilayers. The channel formation of these toxins was extremely inefficient, and in some studies, insertion was not spontaneous and only was achieved mechanically (*3*, *36*). The toxin concentrations needed to observe channel formation under these conditions were 2−3 orders of magnitude higher than their *in vivo* insecticidal concentration. Conductance varied from 11 to 450 pS since multiple subconducting states are frequently observed, showing unstable traces with current jumps of intermediate levels that are difficult to resolve. Under nonsymmetrical ionic conditions, the shift in the zero current voltage (reversal potential E_{rev}) toward the K^+ equilibrium potential (E_K) indicated that channels of Cry1 toxins are cation selective. The data provided in these studies (*14*, *20*, *32*−*35*) are consistent with the data obtained with the pure monomeric Cry1Ab toxin preparation in this work.

On the other hand, studies performed in lipid bilayers containing fused brush border membrane vesicles suggested that the channels formed by Cry1 toxins from Bt in the presence of their receptors have greater conductance than those formed in receptor free bilayers. The conductance of Cry1C-induced channels ranged from 50 pS to 1.9 nS in bilayers containing brush border membranes from *Spodoptera frugiperda* (*18*). Similarly, the conductances of channels induced by Cry1Aa toxin in bilayers containing membranes from *Lymantria dispar* were ∼8-fold larger than the conductances of the channels formed in the absence of the receptor (*36*). However, the presence of multiple conductances is still observed, and the instability of the currents induced in these studies suggested that even in the presence of receptors the insertion of monomers into the membrane does not involve a single conformation. In contrast, currents induced by pure oligomer preparations in the absence of receptor showed highly stable conductances, suggesting a stable insertion of a single conformation of the toxin into the membrane. Single-channel analysis of the pure oligomer in bilayers containing fused receptors will provide more information about the characteristics of the pores formed by Cry toxins under physiological conditions (work in progress).

The oligomeric structure is able to interact with the membrane in contrast to the monomer that has marginal interaction with the liposomes. The partitioning of the oligomeric structure in the membrane is independent of the membrane lipid composition (anionic phosphatidylserine or zwitterionic lipids). However, more changes occur in the Trp fluorescence when the oligomeric structure interacts with model membranes containing anionic lipids. The changes in the intensity of the fluorescence emission spectrum were greater for the oligomer inserted into PC/PS SUV than for the oligomer inserted into SUV prepared with the PC zwitterionic phospholipid alone. The fact that Trp fluorescence modifications are more prevalent when net negative charges are present at the membrane surface suggests that electrostatic attractions of Trp residues incorporated into the lipid bilayer may play important roles in the insertion of toxin into the membrane. There are other examples describing interaction of proteins or peptides with synthetic liposomes with different lipid composition. The fluorescence emission signature of Trp of rhodopsin (*22*), of the human dystrophin rod domain (*23*), and of the peptide temporin L (*24*) increased in intensity, and a blue shift of the maximum emission wavelength was observed in membrane vesicles containing increasing amounts of anionic phospholipids. In all these cases, anionic phospholipids increased the level of insertion of Trp into membranes (*22*−*24*) or stabilized the position of the transmembrane peptide as proven for the TMX-1 peptide, which exhibited an irreversible insertion into liposomes induced by anionic lipids (*25*).

In this work, we analyzed for the first time the structural changes presented by Cry1Ab toxin upon membrane insertion. First, after oligomer formation, some Trp residues are buried within the protein structure. Second, membrane insertion of the oligomeric structure results in further concealing of the Trp residues principally located at the membrane−water interface. However, the precise structure of the toxin in its membrane-inserted state still remains to be determined. Mutagenesis of single Trp residues and analysis of their location in mutant proteins (work in progress) will be helpful in determining the structure of Cry toxins in the membrane-inserted state. Finally, the previous analysis of the *in vitro* pore formation activity of Cry toxins showed that the interaction of the monomeric toxin with the membrane was inefficient. Here we show that the oligomeric structure interacts more efficiently with the membrane, forming stable pores, which is compatible with a pore-forming toxin, as has been postulated for Cry toxins.

ACKNOWLEDGMENT

We acknowledge Jorge Sánchez, Lizbeth Cabrera, Oswaldo López, Claudia Morera, and Jose Luis de la Vega for technical assistance. We thank Dr. Alberto Darszon for providing the facilities of his laboratory.

REFERENCES

1. Schnepf, E., Crickmore, N., Van Rie, J., Lereclus, D., Baum, J., Feitelson, J., Zeigler, D. R., and Dean, D. H. (1998) *Microbiol. Mol. Biol. Rev. 62*, 775−806.
2. Bravo, A., Jansens, S., and Peferoen, M. (1992) *J. Invertebr. Pathol. 60*, 237−246.
3. Hofmann, C., Vanderbruggen, H., Höfte, H., Van Rie, J., Jansens, S., and Van Mellaert, H. (1988) *Proc. Natl. Acad. Sci. U.S.A. 85*, 7844−7848.
4. Jenkins, J. L., and Dean, D. H. (2000) *Genet. Eng. 22*, 33−54.
5. Dorsch, J. A., Candas, M., Griko, N. B., Maaty, W. S. A., Midbo, E. G., Vadlamudi, R. K., and Bulla, L. A., Jr. (2002) *Insect Biochem. Mol. Biol. 32*, 1025−1036.
6. Gómez, I., Sánchez, J., Miranda, R., Bravo, A., and Soberón, M. (2002) *FEBS Lett. 513*, 242−246.
7. Aronson, A., Geng, Ch., and Wu, L. (1999) *Appl. Environ. Microbiol. 65*, 2503−2507.
8. Soberón, M., Perez, R. V., Nuñez-Valdéz, M. E., Lorence, A., Gómez, I., Sánchez, J., and Bravo, A. (2000) *FEMS Microbiol. Lett. 191*, 221−225.
9. Vie, V., Van Mau, N., Pomarede, P., Dance, C., Schwartz, J. L., Laprade, R., Frutos, R., Rang, C., Masson, L., Heitz, F., and Le Grimellec, C. (2001) *J. Membr. Biol. 180*, 195−203.
10. Tigue, J. N., Jacoby, J., and Ellar, D. J. (2001) *Appl. Environ. Microbiol. 67*, 5715−5720.
11. Lakowicz, J. (1983) *Principles of fluorescence spectroscopy*, Plenum Press, New York.
12. Ladokhin, A. S. (1999) *Anal. Biochem. 276*, 65−71.
13. Yau, W.-M., Wimley, W. C., Gawrisch, K., and White, S. H. (1998) *Biochemistry 37*, 14713−14718.
14. Grochulski, P., Masson, L., Borisova, S., Pusztai-Carey, M., Schwartz, J. L., Brousseau, R., and Cygler, M. (1995) *J. Mol. Biol. 254*, 447−464.
15. Arantes, O., and Lereclus, D. (1991) *Gene 108*, 115−119.
16. Thomas, W. E., and Ellar, D. J. (1983) *J. Cell Sci. 60*, 181−197.
17. Müeller, P., Rudin, D. O., Tien, H. T., and Westcott, W. C. (1962) *Nature 194*, 979.
18. Lorence, A., Darszon, A., Díaz, C., Liévano, A., Quintero, R., and Bravo, A. (1995) *FEBS Lett. 360*, 217−222.
19. van der Goot, F. G., Pattus, F., Wong, K. R., and Buckley, J. T. (1993) *Biochemistry 32*, 2636−2642.
20. Schwartz, J. L., Garneau, L., Savaria, D., Masson, L., Brousseau, R., and Rousseau, E. (1993) *J. Membr. Biol. 132*, 53−62.
21. Ladokhin, A. S., Jayasinghe, S., and White, S. H. (2000) *Anal. Biochem. 285*, 235−245.
22. Krishna, G. A., Menon, S. T., Terry, T. J., and Sakmar, T. P. (2002) *Biochemistry 41*, 8298−8309.
23. Le Rumeur, E., Fichou, Y., Pottier, S., Gaboriau, F., Rondeau-Mouro, C., Vincent, M., Gallay, J., and Bondon, A. (2003) *J. Biol. Chem. 278*, 5993−6001.
24. Zhao, H., and Kinnunen, P. K. J. (2002) *J. Biol. Chem. 277*, 25170−25177.
25. Wimley, W. C., and White, S. H. (2000) *Biochemistry 39*, 4432−4442.
26. Burstein, E. A., Vedemkina, N. S., and Ivkova, M. N. (1973) *Photochem. Photobiol. 18*, 263−279.
27. Wimley, W. C., Creamer, T. P., and White, S. H. (1996) *Biochemistry 35*, 5109−5124.
28. Liu, L. P., and Deber, C. M. (1997) *Biochemistry 36*, 5476−5482.
29. Loseva, O. I., Tiktopulo, E. I., Vasiliev, V. D., Nikulin, A. D., Dobritsa, A. P., and Potekhin, S. A. (2001) *Biochemistry 40*, 14143−14151.
30. Caputo, G. A., and London, E. (2003) *Biochemistry 42*, 3265−3274.
31. Raja, S. M., Rawat, S. S., Chattopadhyay, A., and Lala, A. K. (1999) *Biophys. J. 76*, 1469−1479.
32. Schwartz, J. L., Lu, Y.-J., Söhnlein, P., Brousseau, R., Laprade, R., Masson, L., and Adang, M. J. (1997) *FEBS Lett. 412*, 270−276.
33. Slatin, S. L., Abrams, C. K., and English, L. H. (1990) *Biochem. Biophys. Res. Commun. 169*, 765−772.
34. Smedley, D. P., Armstrong, G., and Ellar, D. J. (1997) *Mol. Membr. Biol. 14*, 13−18.
35. Peyronnet, O., Nieman, B., Généreux, F., Vachon, V., Laprade, R., and Schwartz, J.-L. (2002) *Biochim. Biophys. Acta 1567*, 113−122.
36. Peyronnet, O., Vachon, V., Schwartz, J. L., and Laprade, R. (2001) *J. Membr. Biol. 184*, 45−54.

BI035527D